In-situ nanoscale ablation

Thomas J. Cochell*
University of Kentucky, Lexington, KY, 40506

Raymond R. Unocic†
Oak Ridge National Laboratory, Oak Ridge, TN, 37830

Brody K. Bessire‡
NASA Ames Research Center, Moffett Field, CA, 94035

Savio J. Poovanthingal§ and Alexandre Martin¶
University of Kentucky, Lexington, KY, 40506

An understanding of the ablation of carbon-based materials is crucial to modeling the behavior of atmospheric entry spacecrafts equipped with thermal protection systems (TPS). Carbon is the backbone of TPS systems such as PICA (phenolic-impregnated carbon ablator). Therefore in the present work we study ablation of highly oriented pyrolytic graphite (HOPG) in oxygen at temperatures up to 1000°C done within a gas reaction cell housed in a scanning transmission electron microscope (STEM). Observation of the HOPG oxidation on specimens sectioned parallel and normal to the carbon basal planes in the presence of oxygen are reported. Pitting caused by residual oxygen and/or platinum particles from the sectioning process was observed before oxygen gas flow was established at 750 °C in the specimen sectioned with the carbon basal planes parallel to the beam direction. Introduction of oxygen flow caused rapid oxidation moving in a uniform front that completely consumed the HOPG in approximately 1.5 minutes. The specimen sectioned with the carbon basal planes normal to the beam direction did not show the same pitting phenomenon but exhibited rapid oxidation at 1000°C that proceeded in a uniform front and completed in approximately 1 minute. All specimens tested had a husk resembling the original specimen shape left over after oxidation. It is concluded that this husk is most likely ash impurity from the HOPG or impurities from the sectioning process or E-chip. A residual gas analyszer (RGA) was successfully used to monitor gas flows during the experiments but was yet unsuccessful in monitoring oxidation gas products produced during the experiment. Future studies will optimize the RGA setup in order to maximize the potential for detecting these species. These in-situ studies successfully show how this highly ordered carbon ablates on a nano- and micro-scopic length scale and can be used to provide fundamental understanding of carbon ablation that can be used to design the next-generation of TPS systems.

I. Introduction

Atmospheric entry spacecrafts are equipped with thermal protection systems (TPS) to shield the payload from extreme heating. The material used for TPS is usually a composite made of a solid porous matrix and a polymer.[1] One such example is PICA (phenolic-impregnated carbon ablator) which was used for many NASA missions, such as Mars 2020[2]. PICA is a low-density, high-porosity ablative material made of a carbon fiber preform, FiberForm,® impregnated with phenolic resin. During the heating phase of the atmospheric entry, the phenolic rapidly pyrolyzes, with only the charred preform remaining.[3, 4] The exposed carbon fibers interact with the oxygen in the atmosphere – or species containing oxygen, such as CO_2 – and start to oxidize. The ability of the charred carbon fibers to survive the harsh entry conditions is directly linked to the carbon oxidation rates at high temperature and under an oxygen-rich environment.

*Senior Lecturer, Chemical and Materials Engineering, 177 F. Paul Anderson Tower
†Group Leader, Materials Micro-analysis Group, Center for Nanophase Materials Sciences
‡Sr. Scientist, Thermal Protection Materials Branch, Entry Systems and Technology Division, Member AIAA
§Assistant Professor, Mechanical and Aerospace Engineering, 151 Ralph G. Anderson Building, Senior Member AIAA
¶EJ Nutter Professor, Mechanical and Aerospace Engineering, 151 Ralph G. Anderson Building, Associate Member AIAA

From a fundamental standpoint, the chemistry of carbon oxidation remains poorly understood. Decades of research, starting in the 1950's,[5] have yielded global models of carbon oxidation where all the elementary processes are lumped into a few global reactions. Other global models have been developed using chemical equilibrium assumptions, and were verified using high enthalpy experiments[6]. Detailed kinetic mechanisms, including molecular-scale processes, remain elusive despite recent efforts to bridge the gap between microscopic and empirical approaches[7, 8]. More recently, molecular beam experiments have been performed to provide a better understanding of the interaction between the hot carbon char and oxygen.[9, 10]. These experiments have led to the construction of a finite-rate kinetic model based on reaction probabilities.[11, 12] Contrary to previous models which are largely based on empirical measurements,[13, 14] all the individual rates are directly calculated from molecular beam data.

One important aspect of oxidation relates to the evolution of the carbon surface topology, the phenomenon generically called "pitting". Past experimental studies have found that in certain conditions, oxidation does not occur uniformly but takes the form of pits or crater-like cavities, randomly scattered across the otherwise smooth carbon surface.[15–17] These pits initiate at atomic vacancies, defects, or basal plane carbon atoms[17, 18], eventually reaching the scale of the diameter of the fibers.[19] Hahn [18] observed that the frequency, size and initiation sites of the pits on highly oriented pyrolytic graphic (HOPG) varies with temperature. At temperatures of less than 875°C, pits were only initiated by defects, while at higher temperatures, they were also initiated from basal plane layers.

Over the years, two main techniques have been used to perform *in situ* environmental transmission electron microscope (TEM) studies. The first method involves directly introducing gas in the high-vacuum column of a dedicated environmental TEM (ETEM). [20, 21] However, this method severely limits the partial pressure of the reactive gas, as the column must remains at very low pressure. Moreover, the method is not without risks as the TEM column can be contaminated with the reactive gases. A more recent approach makes use of a specially designed closed cell gas reaction gas-cell holder.[22, 23] With this method, the sample is contained within electron transparent silicon nitride membranes and the temperature, pressure and gas environment is controlled. The environment within the gas cell can be controlled by setting: a static gas quantity or gas flow, the temperature from ambient up to 1000°C and the pressure up to 1 atm. Additionally, the layer of gas in the cell is thin, thereby maintaining high spatial resolution. [24]

The surface roughness due to pitting affects the reactive area of the material, and therefore, the net oxidation rate. The current state-of-the-art resorts to *ad hoc* models of surface evolution. [25] Since the onset and propagation of this phenomenon is not fully understood, it is difficult to accurately predict the available reactive area or the oxidation rate. A better understanding of the evolution of pitting on a much smaller length scale is thus needed. The goal of this work is to study the oxidization of carbon at the microstructural-level. Previous work[19, 26] has determined the bulk properties of FiberForm during oxidation in air, O_2 and CO_2. A first set of *in situ* experiments[27] built on that work to illuminate the microstructural-dependent properties of FiberForm and carbon such as the mechanism of pitting as opposed to the bulk properties such as mass loss and recession at given temperatures and reactant flow rates in previous work[19]. To this end, a thin section of FiberForm® was heated in a closed gas-cell under a steady flow of air while being examined in real-time using a scanning transmission electron microscope (STEM). The results of that experiment demonstrated the use of this technique to derive rates, but also highlighted the difficulty of working with FiberForm – a very material that contains carbon under various forms – to obtain general rates. Here, the procedure is repeated in a more controlled manner, using a well characterized and homogeneous carbon material: HOPG.

II. Experimental Procedures

Highly oriented pyrolytic graphite (HOPG) was obtained from SPI Supplies (West Chester, PA, USA). The $10 \times 10 \times 3$ mm^3 piece of HOPG Grade 2 had a mosaic angle of 0.8°, a lateral grain size of 0.5 mm and purity of 99.99%. A FEI Helios Nanolab 660 located in the Electron Microscopy Center at the University of Kentucky was used to mill thin specimens parallel and normal to the carbon basal planes. Briefly, a thin strip of platinum was deposited on top of the HOPG and then the gallium ion beam was to mill on both sides of the strip. The section was attached to the manipulator and lifted out. After attaching to a transmission electron microscope (TEM) grid, the section was further thinned using the ion beam until transparent to electrons. The thin section of HOPG was finally transferred to the Si_xN_y window of a Protochips (Morrisville, NC, USA) Atmosphere E-chip. The section was secured to the SiC surrounding the window in order to provided resistive heating during the experiment.

The E-chip with a thin section of HOPG was then installed into the Atmosphere holder according to manufacturer's instructions in order to create a gas-tight seal that was confirmed using a vacuum chamber up to 1×10^{-6} mbar. The holder was then inserted into a FEI Titan S aberration-corrected scanning TEM (STEM) operating at 300 kV, in the Center for Nanophase Materials Sciences at Oak Ridge National Laboratory. Ar and O_2 (Ultra-high purity, Airgas)

were supplied to the E-chip through the included Atmosphere gas manifold system. Further details on the use of the Protochips Atmosphere setup for studying closed-cell high-temperature gas reactions can be found in Unocic et al. [23]. During the experiment, *in situ* imaging was simultaneously captured in bright-field (BF) and annular dark-field (ADF) imaging modes and video was collected by the integrated Axon Studio software.

A SRS-100 (Sunnyvale, CA, USA) Residual Gas Analyzer was installed downstream of the Atmosphere holder by 0.53 mm inner diameter PEEK tubing to verify gas flow through the E-chip and to observe possible reaction products. The RGA was operated in pressure versus time mode during the experiments monitoring mass-to-charge ratios (m/z) associated with hydrogen, water, nitrogen, oxygen, argon and carbon dioxide.

III. Results

A. Oxidation with Planes Parallel to Beam

The first HOPG section installed in the Atmosphere E-chip for experimentation was sectioned to a thickness of 265 nm at its thickest point and the viewing direction and the electron beam of the STEM were parallel to the carbon basal planes. The E-chip was heated to 750°C in the presence of Ar gas before switching to O_2. Selected bright-field STEM images over the course of the experiment can be found in Fig. 1. Initially the section is 9.7 μm in width and 8.2 μm in height with horizontal lines running across the width indicative of groups of basal planes which can be seen in Fig. 1(a) before the E-chip reached 750°C. Immediately upon the E-chip reaching 750°C the section developed a significant cluster of pits on the bottom portion seen in Fig. 1(b). The development of these pits is interesting as O_2 had not been introduced yet and the RGA showed no detectable levels as indicated by the pressure versus time plot in Fig. 2.

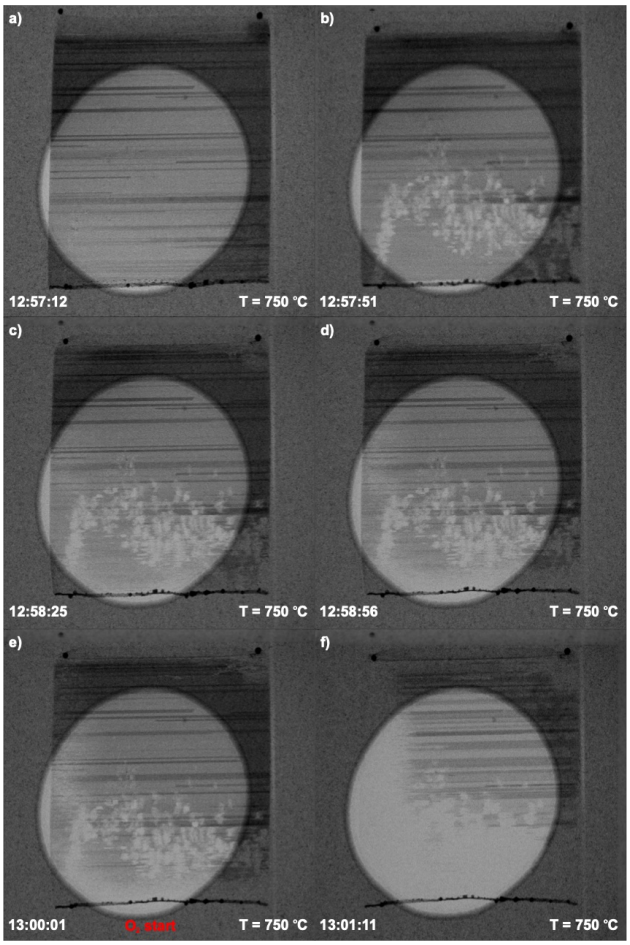

Fig. 1 Selected bright-field STEM images from the oxidation experiment on HOPG segment with carbon basal planes parallel to the electron beam at 750°C.

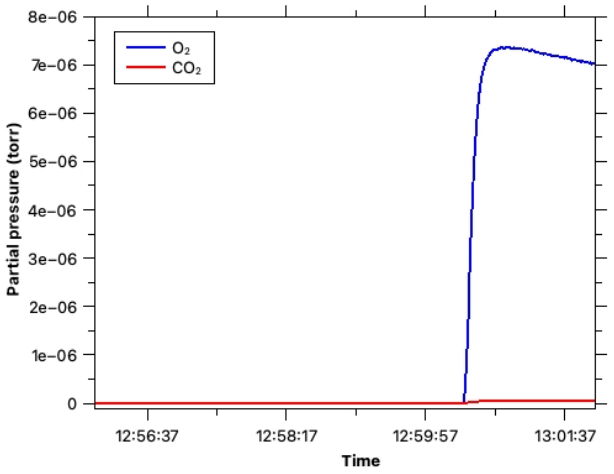

Fig. 2 Pressure versus time plot from the Residual Gas Analyzer downstream of the HOPG segment shown in the previous figure.

It is possible that there is a small amount of O_2 present in the E-chip that is not detected by the RGA or absorbed oxygen on the surface of the carbon that could be responsible for the pitting. The non-uniformity of the pitting suggests there may be a catalytic interaction between the platinum used to adhere the HOPG section to the SiC substrate. The dark dots seen on the corners and bottom surface of the section in FiG. 1 are platinum used during the sectioning and transfer process. There appears to be a streak of pits originating from the bottom left of the image and moving upward toward the center of the HOPG section. It is possible that the platinum on the bottom surface became mobile at the increased temperature. Zhou and Gulari [28] found that platinum thin films deposited on HOPG exhibited morphological changes above 300°C with more significant changes happening at higher temperatures. Another study found that Pt clusters on HOPG transformed into different shapes at 600°C.[29] These mobile Pt nanoparticles could have moved across the surface of the HOPG catalyzing carbon oxidation forming pits along the way. Once the pits were established at 750°C the structure was reasonably stable with no further oxidation observed until O_2 flow began in Fig. 1(e).

Oxygen gas flow was then initiated by the gas manifold software and immediately witnessed by the RGA as seen in Fig. 2. As a result of the flow, oxidation is rapid and moves in a uniform front from the bottom and left of the viewing area. Oxidation takes approximately 1.5 minutes to complete. After which, all that remains is what appears to be a “husk" of the specimen. The husk eventually detaches from the bottom of the window and folds up suggesting that the platinum holding the specimen in place migrated, weakening the adhesion to the SiC substrate around the window.

B. Oxidation with Planes Normal to Beam

The second HOPG section installed in the Atmosphere E-chip for experimentation was sectioned such that the thickest section in the viewing area was 376 nm (top left of Fig. 3) and tapered down to a thickness of 207 nm in the bottom right of the image. The viewing direction and the electron beam of the STEM were normal to the carbon basal planes. The E-chip was heated to 1000°C in the presence of Ar and no noticeable oxidation was observed. Despite the higher temperature compared to the previous experiment, no noticeable migration of platinum or pitting can be observed.

A small flow rate of O_2 was then set with the gas manifold software and verified with RGA. Again, no observable oxidation was present so the flow rate was increased. At this flow rate (panels (a)-(c) in Fig. 3) the effects of oxidation are small but noticeable. Namely, there is a thinning of the bottom right edge of the section indicated by the lighter gray-scale. Additionally, it appears that stacks of carbon basal planes in the HOPG section are being oxidized from the edges towards the top left direction. These stacks are apparent in the heterogeneity of the grey-scale in the thickness of the section.

The flow rate of O_2 was once again increased starting with panel c in Fig. 3. At this flow rate, oxidation was rapid and progressed in a uniform front from the bottom right and bottom left edges towards the top of the section. Oxidation appeared to complete approximately 1 minute later (Fig. 3(f)). Again leaving behind a husk that remained stable with increasing oxygen flow rate.

This phenomenon of a remaining "husk" after oxidation was observed in all experiments regardless of section type.

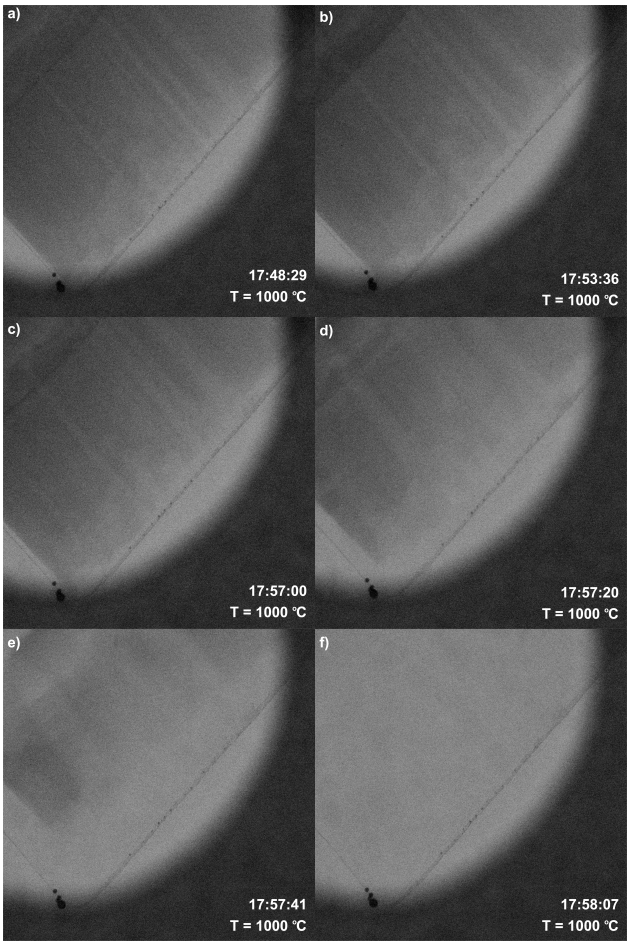

Fig. 3 Selected bright-field STEM images from oxidation experiment on HOPG segment with carbon basal planes normal to the electron beam at 1000°C.

The parallel section from the previous section along with this normal section. Additionally, another normal section specimen demonstrated the husk phenomenon and is shown in Fig. 4. It is unlikely that these husks are remaining un-oxidized carbon. The husk could be ash remaining from the HOPG. The manufacturer reports the purity of this HOPG to be 99.99% with 10 ppm ash. It is also possible that byproducts from the sectioning process (such as Pt or residual gallium) or from the E-chip could contribute to this husk formation. The extremely small amounts of material make it difficult to confirm with post-mortem analysis.

C. Use of Residual Gas Analysis

Finally, the use of RGA was vital to confirming gas flow throughout the oxidation experiments. Fig. 5 shows the partial pressure associated with the m/z ratio for O_2 over the course of an in-situ experiment. During the pumping and purging of the E-chip, 400 s, the O_2 pressure gradually decreases. This step is done before all experiments to remove residual gases in the E-cell. Next, the E-chip is evacuated of all gases to start at vacuum, 550 s. Around 600 s, O_2 flow is established in the E-chip. At 660 s into the experiment, the O_2 flow is increased and then stepped down in order to correlate the gas manifold software to the RGA gas pressure response. This shows that the RGA is sensitive to changes in the gas flow imposed by the manifold software and that the RGA can be used to monitor gas flow in the E-chip. While gas flow imposed by the gas manifold software was readily detected by the RGA, definitive evidence of product gas species from the oxidation such as CO and CO_2 was not found. Future work will be done to optimize the experimental setup of the RGA system in the location downstream of the E-chip. This is to give the best chance to monitor reaction gas products during in-situ STEM experiments.

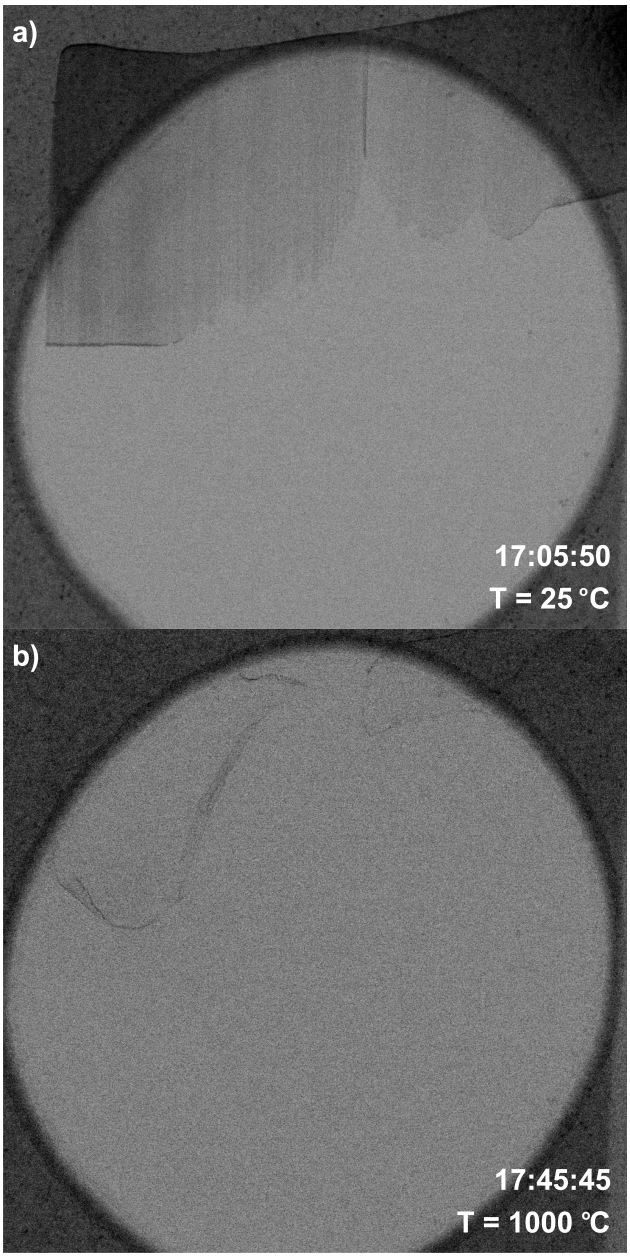

Fig. 4 Bright-field STEM images (a) before and (b) after an oxidation experiment on a HOPG segment with carbon basal planes normal to the electron beam at 1000°C.

IV. Conclusion

First of its kind in-situ observations of HOPG oxidation on specimens sectioned parallel and normal to the carbon basal planes in the presence of oxygen are reported. Pitting caused by residual oxygen and/or platinum particles from the sectioning process was observed before oxygen gas flow was established at 750°C in the specimen sectioned with the carbon basal planes parallel to the beam direction. Introduction of oxygen flow caused rapid oxidation moving in a uniform front that completely consumed the HOPG in approximately 1.5 mintues. The specimen sectioned with the carbon basal planes normal to the beam direction did not show the same pitting phenomenon but exhibited rapid oxidation at 1000°C to proceeded in a uniform front and completed in approximately 1 minute. All specimens tested had a husk resembling the original specimen shape left over after oxidation. It is concluded that this husk is most likely ash impurity from the HOPG or impurities from the sectioning process or E-chip. RGA was successfully used to monitor

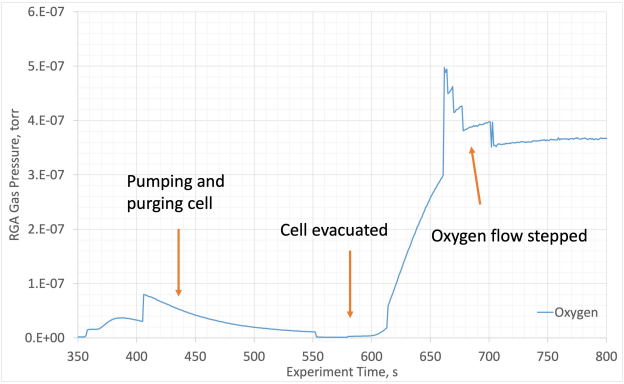

Fig. 5 RGA pressure versus time plot for the HOPG section in Fig. 4 showing the m/z signal for O_2.

gas flows during the experiments but was yet unsuccessful in monitoring oxidation gas products produced during the experiment. Future studies will aim to optimize the RGA setup in order to maximize the potential for detecting these species.

The results presented here shows the possibility of using *in situ* electron microscopic technique to characterize carbon oxidation, and thus a path to providing clean data to validate nano-scale models[30–33].

Acknowledgments

Financial support for this work was provided by NASA STRI Award 80NSSC21K1117. The authors are thankful to N. Briot at the Electron Microscopy Center of the University of Kentucky for the preparation of the samples.

References

[1] Bowman, W. H., and Lawrence, R. M., "Ablative materials for high-temperature thermal protection of space vehicles," *Journal of Chemical Education*, Vol. 48, No. 10, 1971, pp. 690–691. https://doi.org/10.1021/ed048p690.

[2] Hwang, H., Bose, D., Wright, H., White, T. R., Schoenenberger, M., Santos, J., Karlgaard, C. D., Kuhl, C., Oishi, T., and Trombetta, D., "Mars 2020 Entry, Descent, and Landing Instrumentation (MEDLI2)," *46th AIAA Thermophysics Conference*, 2016. https://doi.org/10.2514/6.2016-3536.

[3] Weng, H., Duzel, U., Fu, R., and Martin, A., "Geometric effects on charring ablator: modeling of the full-scale Stardust heat shield," *Journal of Spacecraft and Rockets*, 2020. https://doi.org/10.2514/1.A34828.

[4] Weng, H., and Martin, A., "Numerical Investigation of Thermal Response Using Orthotropic Charring Ablative Material," *Journal of Thermophysics and Heat Transfer*, Vol. 29, No. 3, 2015, pp. 429–438. https://doi.org/10.2514/1.T4576.

[5] Walker, P. L., Rusinko, F., and Austin, L. G., *Gas Reactions of Carbon*, Academic Press, 1959, Vol. 11, pp. 133–221. https://doi.org/10.1016/S0360-0564(08)60418-6.

[6] Milos, F. S., Gasch, M. J., and Prabhu, D. K., "Conformal Phenolic Impregnated Carbon Ablator (C-PICA) Arcjet Testing, Ablation and Thermal Response," *Journal of Spacecraft and Rockets*, Vol. 52, No. 3, 2015, pp. 804–812. https://doi.org/10.2514/1.A33216.

[7] Campbell, P., and Mitchell, R., "The impact of the distributions of surface oxides and their migration on characterization of the heterogeneous carbon–oxygen reaction," *Combustion and Flame*, Vol. 154, No. 1-2, 2008, pp. 47–66. https://doi.org/10.1016/j.combustflame.2007.11.002.

[8] Du, Z., Sarofim, A. F., Longwell, J. P., and Mims, C. A., "Kinetic measurement and modeling of carbon oxidation," *Energy and Fuels*, Vol. 5, No. 1, 1991, pp. 214–221. https://doi.org/10.1021/ef00025a035.

[9] Paci, J. T., Upadhyaya, H. P., Zhang, J., Schatz, G. C., and Minton, T. K., "Theoretical and Experimental Studies of the Reactions Between Hyperthermal O(3P) and Graphite: Graphene-Based Direct Dynamics and Beam-Surface Scattering Approaches," *Journal of Physical Chemistry A*, Vol. 113, No. 16, 2009, pp. 4677–4685. https://doi.org/10.1021/jp9000412.

[10] Murray, V. J., Marshall, B. C., Woodburn, P. J., and Minton, T. K., "Inelastic and Reactive Scattering Dynamics of Hyperthermal O and O2 on Hot Vitreous Carbon Surfaces,," *Journal of Physical Chemistry C*, Vol. 119, No. 26, 2015, pp. 14,780–14,796. https://doi.org/10.1021/acs.jpcc.5b00924.

[11] Poovathingal, S., Schwartzentruber, T. E., Murray, V. J., and Minton, T. K., "Molecular Simulations of Surface Ablation Using Reaction Probabilities from Molecular Beam Experiments and Realistic Microstructure," *AIAA Journal*, Vol. 54, No. 1, 2016, pp. 1–11. https://doi.org/10.2514/1.J054903.

[12] Poovathingal, S., Schwartzentruber, T. E., Murray, V. J., Minton, T. K., and Candler, G. V., "Finite-Rate Oxidation Model for Carbon Surfaces from Molecular Beam Experiments," *AIAA Journal*, 2017, pp. 1–15. https://doi.org/10.2514/1.j055371.

[13] Park, C., "Effects of Atomic Oxygen on Graphite Ablation," *AIAA Journal*, Vol. 14, No. 11, 1976, pp. 1640–1642. https://doi.org/10.2514/3.7267.

[14] Zhluktov, S. V., and Abe, T., "Viscous Shock-Layer Simulation of Airflow past Ablating Blunt Body with Carbon Surface," *Journal of Thermophysics and Heat Transfer*, Vol. 13, No. 1, 1999, pp. 50–59. https://doi.org/10.2514/2.6400.

[15] Helber, B., Chazot, O., Hubin, A., and Magin, T. E., "Microstructure and gas-surface interaction studies of a low-density carbon-bonded carbon fiber composite in atmospheric entry plasmas," *Composites Part A: Applied Science and Manufacturing*, Vol. 72, 2015, pp. 96–107. https://doi.org/10.1016/j.compositesa.2015.02.004.

[16] Miller-Oana, M., "Oxidation Behavior of Carbon and Ultra-High Temperature Ceramics," Ph.D. thesis, University of Arizona, Tucson, AZ, 2016. https://doi.org/10150/605121.

[17] Chang, H., and Bard, A. J., "Scanning tunneling microscopy studies of carbon-oxygen reactions on highly oriented pyrolytic graphite," *Journal of the American Chemical Society*, Vol. 113, No. 15, 1991, pp. 5588–5596. https://doi.org/10.1021/ja00015a012.

[18] Hahn, J., "Kinetic study of graphite oxidation along two lattice directions," *Carbon*, Vol. 43, No. 7, 2005, pp. 1506 – 1511. https://doi.org/10.1016/j.carbon.2005.01.032.

[19] Panerai, F., Cochell, T. J., Martin, A., and White, J. D., "Experimental measurements of the high-temperature oxidation of carbon fibers," *International Journal of Heat and Mass Transfer*, Vol. 136, 2019, pp. 972–986. https://doi.org/10.1016/j.ijheatmasstransfer.2019.03.018.

[20] Wang, C.-M., Genc, A., Cheng, H., Pullan, L., Baer, D. R., and Bruemmer, S. M., "In-Situ TEM visualization of vacancy injection and chemical partition during oxidation of Ni-Cr nanoparticles," *Scientific Reports*, Vol. 4, 2014. https://doi.org/10.1038/srep03683, article number 3683.

[21] Jeangros, Q., Hansen, T. W., Wagner, J. B., Dunin-Borkowski, R. E., Hebert, C., Hessler-Wyser, J., Hébert, C., herle, J. V., and Hessler-Wyser, A., "Reduction of nickel oxide particles by hydrogen studied in an environmental TEM," *Acta materialia*, Vol. 67, 2014, pp. 362–372. https://doi.org/10.1016/j.actamat.2013.12.035.

[22] Allard, L. F., Bigelow, W. C., Wu, Z., Overbury, S. H., Unocic, K. A., Chi, M., Carpenter, W. B., Walden, F. S., Thomas, R. L., Gardiner, D. S., and et al., "Computer-Controlled In Situ Gas Reactions via a MEMS-based Closed-Cell System," *Microscopy and Microanalysis*, Vol. 21, No. S3, 2015, pp. 97–98. https://doi.org/10.1017/S1431927615001282.

[23] Unocic, K. A., Shin, D., Unocic, R. R., and Allard, L. F., "NiAl Oxidation Reaction Processes Studied In Situ Using MEMS-Based Closed-Cell Gas Reaction Transmission Electron Microscopy," *Oxidation of Metals*, Vol. 88, No. 3-4, 2017, pp. 495–508. https://doi.org/10.1007/s11085-016-9676-2.

[24] de Jonge, N., Houben, L., Dunin-Borkowski, R. E., and Ross, F. M., "Resolution and aberration correction in liquid cell transmission electron microscopy," *Nature Reviews Materials*, Vol. 4, No. 1, 2019, pp. 61–78. https://doi.org/10.1038/s41578-018-0071-2.

[25] Bhatia, S. K., and Perlmutter, D. D., "A random pore model for fluid-solid reactions: I. Isothermal, kinetic control," *AIChE Journal*, Vol. 26, No. 3, 1980, pp. 379–386. https://doi.org/10.1002/aic.690260308.

[26] Panerai, F., Martin, A., Mansour, N. N., Sepka, S. A., and Lachaud, J., "Flow-Tube Oxidation Experiments on the Carbon Preform of a Phenolic-Impregnated Carbon Ablator," *Journal of Thermophysics and Heat Transfer*, Vol. 27, No. 2, 2014, pp. 181–190. https://doi.org/10.2514/1.T4265.

[27] Cochell, T. J., Unocic, R. R., Grana-Otero, J., and Martin, A., "Nanoscale oxidation behavior of carbon fibers revealed with in situ gas cell STEM," *Scripta Materialia*, Vol. 199, 2020. https://doi.org/10.1016/j.scriptamat.2021.113820, article 113820.

[28] Zhou, X. C., and Gulari, E., "Scanning tunneling microscopy of the annealing of a thin platinum film on highly oriented pyrolytic graphite," *Acta Crystallographica Section A*, Vol. 47, No. 1, 1991, pp. 17–21. https://doi.org/10.1107/S0108767390009060, URL https://doi.org/10.1107/S0108767390009060.

[29] Lee, S., Permana, H., and Simon Ng, K., "Effects of annealing and gas treatment on the morphology of platinum cluster size on highly oriented pyrolytic graphite by scanning tunneling microscopy," *Catalysis letters*, Vol. 23, 1994, pp. 281–292.

[30] Schmitt, S., and Martin, A., "A Kinetic Monte Carlo based analysis of graphite oxidation with realistic defect distributions," *AIAA Aviation Forum*, Chicago, IL, 2022. https://doi.org/10.2514/6.2022-3945.

[31] Schmitt, S., and Martin, A., "Extension of Kinetic Monte Carlo Simulation Framework to Multilayer Graphene and Graphite Oxidation," *AIAA SciTech Forum*, San Diego, CA, 2022. https://doi.org/10.2514/6.2022-1284.

[32] Schmitt, S., and Martin, A., "Kinetic Monte Carlo Simulations of Nitrogen-Carbon Gas-Surface Reaction at High Temperatures," *AIAA SciTech Forum*, San Diego, CA, 2022. https://doi.org/10.2514/6.2022-0113.

[33] Edward, S., and Johnson, H. T., "Oxidation of Multi-layer Graphite Using an Atomistic Multi-lattice Kinetic Monte Carlo Model," *The Journal of Physical Chemistry C*, Vol. 34, 127, pp. 16938–16949. https://doi.org/10.1021/acs.jpcc.3c04865.